



CHORUS

This is the accepted manuscript made available via CHORUS. The article has been published as:

Symmetry-conserving purification of quantum states within the density matrix renormalization group

A. Nocera and G. Alvarez

Phys. Rev. B **93**, 045137 — Published 28 January 2016

DOI: [10.1103/PhysRevB.93.045137](https://doi.org/10.1103/PhysRevB.93.045137)

Symmetry Conserving Purification of Quantum States within the Density Matrix Renormalization Group

A. Nocera and G. Alvarez

*Computer Science & Mathematics Division and Center for Nanophase Materials Sciences,
Oak Ridge National Laboratory, Oak Ridge, Tennessee 37831, USA*

The density matrix renormalization group (DMRG) algorithm was originally designed to efficiently compute the zero temperature or ground-state properties of one dimensional strongly correlated quantum systems. The development of the algorithm at finite temperature has been a topic of much interest, because of the usefulness of thermodynamics quantities in understanding the physics of condensed matter systems, and because of the increased complexity associated with efficiently computing temperature-dependent properties. The ancilla method is a DMRG technique that enables the computation of these thermodynamic quantities. In this paper, we review the ancilla method, and improve its performance by working on reduced Hilbert spaces and using canonical approaches. We furthermore explore its applicability beyond spins systems to t-J and Hubbard models.

PACS numbers: 05.10.Cc 71.10.Fd 71.27.+a 74.25.Bt

I. INTRODUCTION

The behavior of low dimensional strongly correlated electron systems at finite temperature has become a topic of great interest amongst the condensed matter physics community. Tuning the temperature can lead to interesting phenomena which cannot be fully understood in terms of ground state physics, such as the quantum critical regime,¹ the transition to a spin incoherent Luttinger liquid,² or the sudden emergence of a single spinon dispersion in XXZ-like spin-chain materials.³⁻⁵ On the experimental front, recent advances⁶⁻⁹ have enabled very precise measurements of both static and dynamical correlation functions. These experimental results are challenging the available theoretical and computational techniques,¹⁰⁻¹² increasing demand to develop efficient and accurate numerical methods for the investigation and eventual prediction of the thermodynamic quantities.

In one dimension, the density matrix renormalization group¹³⁻¹⁵ (DMRG) is the most powerful method to calculate ground state properties of strongly correlated systems. The DMRG has been successfully extended to treat real time dynamics¹⁶⁻¹⁹ and systems at finite temperature. These extensions include transfer-matrix DMRG,²⁰ minimally entangled typical thermal states or METTS,²¹⁻²³ and the purification scheme^{16,20,24-29} to be used in this paper.

METTS was recently introduced by White in ref. 21, where he shows that these so-called minimally entangled typical thermal states efficiently represent the thermal properties of the system of interest. METTS has been applied to fermionic systems by one of us.³⁰ Ref. 31 compares the purification scheme to the METTS method, concluding that METTS is, in general, computationally less efficient than purification. In particular, it is argued,³¹ that the additional statistical error source introduced by METTS sampling increases computational costs, especially at high temperatures. More recently,

ref. 32 develops symmetry conserving METTS, improving the efficiency of the method. Perhaps METTS and ancilla should be regarded as complementary. Given these recent developments in DMRG techniques for temperature dependence, the present paper revisits the ancilla method, with an emphasis on improving its performance, and exploring its applicability beyond spins systems to t-J and Hubbard models.

The ancilla method was originally introduced within a thermofield formalism by Umezawa³³, and later in DMRG^{16,27}. It is designed to calculate the finite temperature quantum average of an observable, by definition a trace over all the eigenstates of the physical chain, and not accessible with standard DMRG. To this aim, the above quantity is expressed as a quantum average over a pure state—a thermal vacuum—in an enlarged Hilbert space. The Hilbert space is enlarged by adding an ancilla site to each site of the physical lattice, thus obtaining a two-leg ladder geometry. The ancilla’s degrees of freedom are added in such a way that the reduced density matrix of the physical sites reproduces the thermal density matrix.

The purification scheme starts with an infinite temperature state, given by a product of maximally entangled states on each rung of the ladder. For spin chains,¹⁶ each ancilla can be chosen to have “opposite” quantum numbers to those of the corresponding physical site. This choice of ancillas is equivalent to applying a time-reversal transformation in the case of spin chains, or, more generally, a particle-hole transformation on the ancillas, and has its profound motivation in giving the correct Kubo-Martin-Schwinger relations³³⁻³⁶ at finite temperature. The previously described choice has the additional advantage of reducing the dimension of the Hilbert space of the total system composed of physical and ancilla chains. For example, in the case of a Heisenberg model in the absence of a magnetic field, one is able to work in a subspace of the enlarged Hilbert space of physical plus ancilla chains with z component of the total spin equal to zero. After the preparation of the initial state,

a finite temperature state is then obtained by evolving in imaginary time with the Hamiltonian of the physical chain.

In this paper we show that the above approach, which we define as *grand canonical* for the physical chain, is not the most efficient for the DMRG numerical simulations: the preparation of the initial infinite temperature state and the subsequent imaginary time evolution can be furthermore restricted, without any additional truncation of the Hilbert space, to a subspace where the z component of the total spin of the physical chain is *also* conserved. This subspace has clearly smaller dimension than the one previously mentioned, the one that conserves *only* the z component of the total (physical plus ancilla) system.

How can we impose the restriction outlined above? Or, more generally, how can we work in the *canonical ensemble* for the physical chain? To answer this question we will show how to engineer an “entangler” Hamiltonian that conserves a given set of quantum numbers of the physical chain, and generates a maximally entangled infinite temperature state that is different from the state used in the grand canonical approach. Introduced by Feiguin and Fiete in ref. 25 for a t-J chain, it turns out that the canonical “entangler” Hamiltonian is non-local for the total system, but involves interactions between the rungs of the total system at all possible distances. *In the thermodynamic limit*, the canonical scheme gives the same results as the grand canonical one. Yet the performance of the DMRG simulation is remarkably improved, by up to one order of magnitude with respect to the grand canonical approach.

Section II A introduces the grand canonical and the canonical purification schemes for the Heisenberg model. Section II B then extends the treatment to the case of the t-J model, and section II C to the Hubbard model. The Heisenberg model has only spin degrees of freedom, but the t-J and Hubbard models have also charge, leading to different “entangler” Hamiltonians. For each model, we first consider a local *entangler*, where neither the total number of electrons, nor the total number of spins of the physical chain are conserved; they are conserved only in average at finite temperature. This is the *grand canonical ensemble*. It needs a (temperature-dependent) chemical potential in order to keep constant the *average* number of electrons in the physical chain. A magnetic field is likewise needed to keep constant the *average* z component of the total spin (as in the case of a spin chain). We then consider a non local *entangler* where the number electrons is conserved but not the z -component of the spin. Even in this case, we show that the z -component of the spin for the electrons in the physical chain is conserved in average during the temperature evolution; its value is zero in the absence of a magnetic field. Finally, we write down an entangler such that *both* the number of electrons *and* the z -component of the spin of the physical chain are conserved.

II. THE ANCILLA METHOD FOR FINITE TEMPERATURE DMRG

For convenience, we here summarize the ancilla approach for finite temperature DMRG; refs. 16,37 have more detail. At $\beta = 0$, that is, at infinite temperature, a maximally entangled state $|\psi(\beta = 0)\rangle$ between the physical sites of the chain and their ancillas is initially produced. A pure state in the enlarged system at finite temperature is then calculated by evolving $|\psi(\beta = 0)\rangle$ in imaginary time with the Hamiltonian of the physical sites, $|\psi(\beta)\rangle = e^{-\beta H/2}|\psi(\beta = 0)\rangle$. Given a generic observable O of the physical chain, the thermodynamic average can be calculated^{16,33–36} in the enlarged space using the standard zero temperature expression

$$\langle O \rangle = \frac{\langle \psi(\beta) | O | \psi(\beta) \rangle}{\langle \psi(\beta) | \psi(\beta) \rangle}, \quad (1)$$

where the norm $Z(\beta) = \langle \psi(\beta) | \psi(\beta) \rangle$ represents the partition function at temperature $T \equiv 1/\beta$.

We present two different purification schemes for the initial infinite temperature state. The first scheme is referred to as “grand canonical,” where one conserves only quantum numbers for the enlarged system given by the physical and the ancilla sites. In the second scheme, one conserves quantum numbers *not just* globally, that is, not just in the enlarged system, but in the physical and ancilla chains separately as well.

In the next sections we will often discuss intensive energies of the models considered. The definition of intensive energy is

$$\langle E \rangle / L = \frac{1}{L} \frac{\langle \psi(\beta) | H | \psi(\beta) \rangle}{\langle \psi(\beta) | \psi(\beta) \rangle}, \quad (2)$$

where H is the Hamiltonian of the model under consideration and L is the system size.

A. Heisenberg model

1. Grand-canonical purification scheme

Let us start considering the case of a spin chain described by the Heisenberg model

$$H_{Heis} = J \sum_{i=0}^{L-2} \vec{S}_i \cdot \vec{S}_{i+1}, \quad (3)$$

with $\vec{S} = (S^x, S^y, S^z)$, and where the Hilbert space of a single site is two-dimensional, having only two possible states, $|\uparrow\rangle$ and $|\downarrow\rangle$. Recall briefly the purification scheme adopted in ref. 16, which in our classification turns out to have a grand-canonical character. For simplicity, first consider the case of two spins, accompanied by their ancilla sites. The infinite temperature state is

$$|\psi_{2 \text{ spins}}(\beta = 0)\rangle = \frac{1}{2} (|\uparrow\downarrow\rangle + |\downarrow\uparrow\rangle) \otimes (|\uparrow\downarrow\rangle + |\downarrow\uparrow\rangle), \quad (4)$$

where \otimes is the direct product of states on the two *composite* sites, each given by a pair consisting of a physical site and its ancilla. In this paper, *the first entry of the ket vector refers to the state of the physical site and the second entry to the ancilla site*. For example, ket $|\uparrow\downarrow\rangle$, has a spin up in the physical site and a spin down in the corresponding ancilla site. In the state Eq. (4), each ancilla has “opposite” quantum numbers with respect to those of the physical site. As long as the mapping between the states of a physical site and its ancilla is one-to-one, then any choice for the mapping of quantum numbers of the ancillas yields the correct thermodynamics for the physical chain.

The choice outlined above (which is equivalent to applying a time-reversal transformation¹⁶) has the advantage of reducing the dimension of the Hilbert space of the total enlarged system. By construction, the state Eq. (4) lives in the subspace with spin $S_{\text{tot}}^z \equiv \sum_i (S_i^z + S_{a(i)}^z) = 0$ of the total physical-plus-ancilla Hilbert space, where we have indicated with $a(i)$ the ancilla site corresponding to the physical site i . For L sites, Eq. (4) generalizes to a so-called product of *local* maximally-entangled states

$$|\psi(\beta = 0)\rangle = \frac{1}{\sqrt{\mathcal{N}}} \bigotimes_{i=0}^{L-1} \sum_{\sigma=\uparrow,\downarrow} |\sigma\bar{\sigma}\rangle, \quad (5)$$

where \mathcal{N} is a normalization constant, $\bar{\uparrow} = \downarrow$ and $\bar{\downarrow} = \uparrow$. The above state is an eigenstate of the z -component of the total spin S_{tot}^z , but *it is not* an eigenstate of the total spin of either the physical $S_{\text{ph}}^z \equiv \sum_i S_i^z$ or ancilla sites $S_{\text{an}}^z \equiv \sum_i S_{a(i)}^z$.

The above observation has important consequences for the efficiency of the finite temperature evolution. Indeed, within the purification scheme outlined above, one can study the thermodynamics of a generic spin chain Hamiltonian in the presence of an external magnetic field. The average magnetization of the system can be tuned by changing the strength of the field at finite temperature. This possibility stems from the symmetry property of the initial infinite temperature state, which conserves neither S_{ph}^z , nor S_{an}^z .

A state like Eq. (5) is exponentially large, and would have to be truncated before time evolving it. Otherwise, one would have to work with a vector of size 2^L . For the grand canonical scheme, one could build it by growing it slowly inside a traditional DMRG, and truncating it along the way. But due to the DMRG transformations, the book keeping of such a state would be unfeasible to perform. It is then clear that with traditional DMRG the entangler is needed for an efficient representation of the state. With an MPS approach, the infinite temperature state in Eq. (5) has bond dimension 2, and is not entangled in a global sense, because it is just a product state of singlets on each rung. How can we then generate state Eq. (5) as a starting point for the temperature evolution? As proposed by Feiguin and Fiete in ref. 25, we find useful the notion of “entangler” Hamiltonian: a Hamiltonian having the state Eq. (5) as its ground state.

By diagonalizing a 4×4 matrix, where 4 is the dimension of the composite physical plus ancilla site, the entangler for the Heisenberg model in the grand-canonical scheme can be written as

$$H_{\text{GC}}^{\text{spin}} = - \sum_{i=0}^{L-1} S_i^+ S_{a(i)}^- + \text{h. c.} \quad (6)$$

We address the results coming from this entangler in the next section, where we compare the grand canonical and canonical purification schemes.

2. Canonical purification scheme

Let us consider the case of the Heisenberg model in the absence of a magnetic field. In this case, one would build a maximally entangled state with the property that $S_{\text{tot}}^z |\phi\rangle = 0$, $S_{\text{ph}}^z |\phi\rangle = 0$, $S_{\text{an}}^z |\phi\rangle = 0$, such that one conserves the spin of the physical and ancilla chains *separately*.

For the simple case of two spins, a maximally entangled state with the above characteristics is

$$|\phi_{2 \text{ spins}}(\beta = 0)\rangle = \frac{1}{\sqrt{2}} (|\uparrow\downarrow\rangle \otimes |\downarrow\uparrow\rangle + |\downarrow\uparrow\rangle \otimes |\uparrow\downarrow\rangle). \quad (7)$$

For L sites

$$|\psi(\beta = 0)\rangle_{\text{C}} = \frac{1}{\sqrt{\mathcal{N}'}} P_{(S_{\text{ph}}^z = 0)} \left[\bigotimes_{i=0}^{L-1} \sum_{\sigma=\uparrow,\downarrow} |\sigma\bar{\sigma}\rangle \right], \quad (8)$$

where \mathcal{N}' is a normalization constant, $P_{(S_{\text{ph}}^z = 0)}$ is the projector operator such that the z -component of the *total* spin of the physical (ancilla) chain is conserved and equal to zero: $S_{\text{ph}}^z |\psi(\beta = 0)\rangle_{\text{C}} = S_{\text{an}}^z |\psi(\beta = 0)\rangle_{\text{C}} = 0$.

For an L site chain, the subspace containing the maximally entangled state in the canonical approach has dimension $C_{L/2}^L$ (C_l^k gives the number of possible combinations of l objects on k places), a number clearly smaller than the analogous subspace dimension C_L^{2L} of the grand canonical case. As will be seen below, imposing the conservation of S_{ph}^z , during the finite temperature evolution in the enlarged Hilbert space substantially reduces the computational effort of the time dependent DMRG simulations.³⁸ Conserving this symmetry can thus help improve DMRG implementations, because they usually consider *global* symmetries only.

How can we, in practice, generate the maximally entangled “canonical” state Eq. (8)? By finding the correct “entangler” Hamiltonian, the one that gives Eq. (8) as its ground state. For the Heisenberg model, this “entangler” Hamiltonian is

$$H_{\text{C}}^{\text{spin}} = - \sum_{i \neq j} \Gamma_i^\dagger \Gamma_j + \text{h. c.}, \quad (9)$$

where $\Gamma_i^\dagger = S_i^+ S_{a(i)}^-$. Notice that the above Hamiltonian has long-range interactions: each rung interacts with all

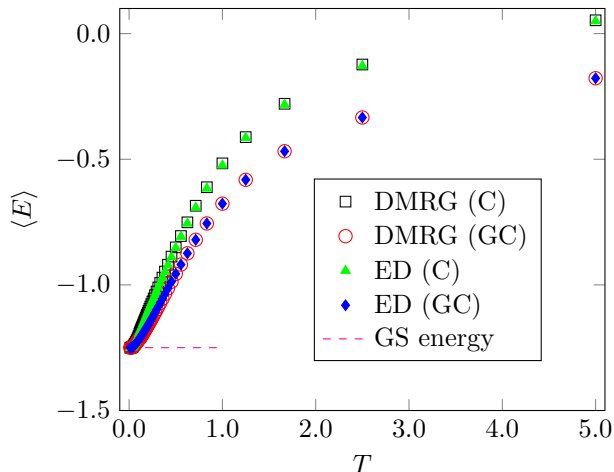


FIG. 1: (Color online) Intensive energies for a Heisenberg chain with $J = -1$ and length $L = 6$ sites for the canonical and grand canonical approach, and comparing DMRG and ED, as indicated.

the others. Section III discusses the entanglement implications caused by long-range interactions in the DMRG calculations. A proof that the state (8) is the ground state of the Hamiltonian (9) is provided in appendix B.

In matrix product operator notation,¹⁵ $H_C^{spin} = \hat{W}^{[0]}\hat{W}^{[1]}\dots\hat{W}^{[L-1]}+\text{h.c.}$, where

$$\hat{W}^{[i]} = \begin{bmatrix} I & 0 & \Gamma_i^\dagger \\ 0 & I & 0 \\ 0 & \Gamma_i & I \end{bmatrix}, \quad (10)$$

for $0 < i < L - 1$, $\hat{W}^{[0]} = [I, 0, \Gamma_0^\dagger]$, and

$$\hat{W}^{[L-1]} = \begin{bmatrix} 0 \\ I \\ \Gamma_{L-1} \end{bmatrix}. \quad (11)$$

Fig. 1 shows the intensive energy defined as a function of the temperature for an antiferromagnetic Heisenberg chain with $L = 6$ sites, and where we assume $|J| = 1$ as unit of energy. Fig. 1 compares both purification schemes. It also compares DMRG with exact diagonalization. The figure shows a perfect numerical agreement between DMRG and ED, but substantially different results between the grand canonical and canonical approaches; the intensive energies calculated within the canonical approach are systematically bigger than those calculated in the grand canonical scheme. Fig. 1 also shows that the results obtained with different approaches coincide for $\beta \rightarrow \infty$, that is, at zero temperature. In appendix A, we prove that for a generic interacting quantum system the canonical (when chosen in a symmetry sector containing the ground state) and grand canonical average energies differ in general, but

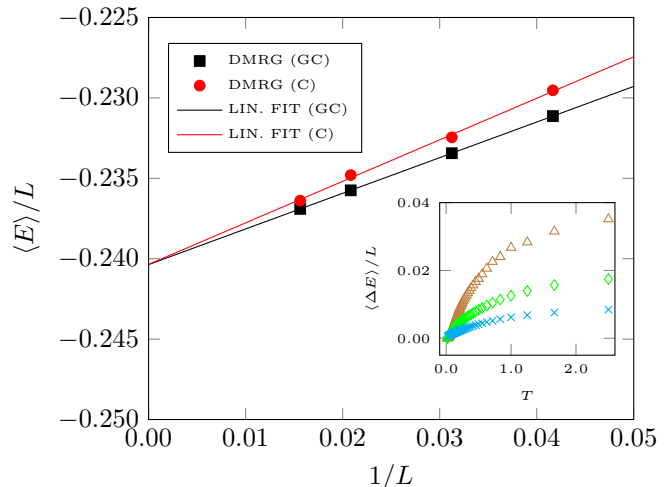


FIG. 2: (Color online) Main panel: average intensive energies for the Heisenberg model ($J = -1$) at temperature $T = 0.1$ as a function of the system size comparing the canonical and the grand canonical approaches (we consider up to $L = 64$ sites). The Bethe ansatz yields an energy equal to -0.240219 in the thermodynamic limit. Inset: difference between the intensive energies obtained in the two approaches, $\langle \Delta E \rangle = \langle E_C \rangle - \langle E_{GC} \rangle$, as function of the temperature, for different system sizes: triangles (brown) indicate $L = 6$, diamonds (green) indicate $L = 12$, and crosses (cyan) indicate $L = 24$.

coincide at zero temperature, and in the thermodynamic limit (where they coincide at any temperature).

The DMRG implementation used throughout this paper is discussed in the supplemental material.³⁹ The algorithm implemented for the time-dependent part of the DMRG is based on the Krylov space decomposition method, as explained in ref. 40 and references therein. An implementation can be found in ref. 41. In the time-evolution calculations, 600–800 states per block are kept. The results are well converged with this number of states in the entire interval of temperature investigated ($\beta_{min} = 0$, $\beta_{max}/2 = 40$, with $\Delta\beta/2 = 0.1$).

Fig. 2 substantiates another analogy of the results obtained in the two purification schemes with those obtained in different ensembles. The main plot of fig. 2 shows the average energies obtained in the canonical and grand canonical approaches as a function of the system size at low temperature, $T = 0.1$. The results are different for small system size, but they converge to the exact Bethe ansatz solution when extrapolated to the thermodynamic limit. The inset shows the difference between the average energies in the grand canonical and canonical approaches, which decreases at *every* temperature with increasing system size. On the other end, all the curves converge to the same value for $\beta \rightarrow \infty$, as already observed in fig. 1. In the supplemental material,³⁹ we have proved that this is valid for a generic quantum system when the thermodynamic limit is taken.

B. t-J chains

1. Grand canonical purification scheme

In this section, we apply the theory discussed previously to the case of a $t - J$ model described by the standard Hamiltonian

$$H_{tJ} = -t \sum_{i=0, \sigma}^{L-2} (c_{i, \sigma}^\dagger c_{i+1, \sigma} + h.c.) + J \sum_{i=0}^{L-2} (\vec{S}_i \cdot \vec{S}_{i+1} - N_i N_{i+1}/4), \quad (12)$$

where $N_i = \sum_{\sigma=\uparrow, \downarrow} c_{i, \sigma}^\dagger c_{i, \sigma}$. The model is characterized by a three-dimensional single-site Hilbert space with states empty $|0\rangle$, single occupied with spin up $|\uparrow\rangle$, and spin down $|\downarrow\rangle$. We start with the grand-canonical purification scheme. Following the same procedure introduced in the spin chains' case, one can straightforwardly write down a product of local (along the rungs of the ladder) maximally entangled states:

$$|\psi(\beta = 0)\rangle = \bigotimes_{i=0}^{L-1} \left[|0, 0\rangle + \sum_{\sigma=\uparrow, \downarrow} |\sigma\bar{\sigma}\rangle \right]. \quad (13)$$

We have verified (by diagonalizing a 9×9 matrix, where 9 is the dimension of a composite physical-plus-ancilla site) that this state can be generated by calculating the ground state of the entangler Hamiltonian

$$H_{GC}^{t-J} = \sum_{i=0}^{L-1} (\sqrt{2}\Delta_i + S_i^+ S_{a(i)}^-) + h. c., \quad (14)$$

where $\Delta_i^\dagger = (c_{i, \uparrow}^\dagger c_{a(i), \downarrow}^\dagger - c_{i, \downarrow}^\dagger c_{a(i), \uparrow}^\dagger)/\sqrt{2}$. As observed in the case of the spin chains, even though Eq. (13) conserves the total spin in the enlarged physical plus ancilla combined system, it *does not conserve these quantities separately* for the physical chain or for the ancilla chain. In order to get the thermodynamic properties for the physical chain at finite temperature in the grand canonical ensemble, one must add a chemical potential term μ during the imaginary time evolution. To keep an average of N electrons in the physical chain, one needs to solve the equation

$$\langle \psi(\beta, \mu) | N_{\text{ph.}} | \psi(\beta, \mu) \rangle = N, \quad (15)$$

for each temperature $T = 1/\beta$, where $|\psi(\beta, \mu)\rangle = e^{-\beta/2[H_{tJ} - \mu N_{\text{ph.}}]} |\psi(\beta = 0)\rangle$, with H_{tJ} being the standard $t - J$ Hamiltonian and $N_{\text{ph.}} \equiv \sum_i N_{i, \text{ph.}}$. For this reason, when studying the thermodynamic properties of the t-J model at fixed density and zero magnetic field, the grand canonical scheme outlined above has a clear disadvantage in terms of computational cost. Therefore, results in the grand canonical scheme are calculated only with exact diagonalization for a small system size. We have verified

that the average spin of the physical chain is zero at any temperature, $\langle \psi(\beta, \mu) | S_{\text{ph.}}^z | \psi(\beta, \mu) \rangle = 0$, with μ being a solution of Eq. (15).

2. Canonical purification scheme

In this section, we address the ‘‘canonical’’ purification scheme for the $t - J$ model. We present two different schemes which take into account the charge and the spin symmetries of the physical chain. We first review a canonical purification method where one only employs the charge conservation in the physical chain. This scheme has already been treated by Feiguin and Fiete in ref. 25 in the context of a spin-incoherent Luttinger liquid. We consider a t-J chain with L sites, and an even number of electrons N , such that $N_\uparrow = N_\downarrow = N/2$. Notice that in the total system given by physical and ancilla sites one has $2N$ electrons. Up to a constant, we here provide the expression

$$|\psi(\beta = 0)\rangle_{C_1} = P_{(N_{\text{ph.}}=N)} \left[\bigotimes_{i=0}^{L-1} (|0, 0\rangle + \sum_{\sigma=\uparrow, \downarrow} |\sigma\bar{\sigma}\rangle) \right] \quad (16)$$

for the ‘‘canonical’’ maximally entangled state in the L sites case, where $P_{(N_{\text{ph.}}=N)}$ is a projector operator (different from the projector that appears in Eq. (8)) such that the total number of electrons of the physical (ancilla) chain is conserved, $N_{\text{ph.}} |\psi(\beta = 0)\rangle_{C_1} = N_{\text{an.}} |\psi(\beta = 0)\rangle_{C_1} = N$. We emphasize that the above state does *not* conserve the z -component of the total spin of the physical (ancilla) chain, but it has the property that, at any temperature, ${}_{C_1} \langle \psi(\beta) | S_{\text{ph.}}^z | \psi(\beta) \rangle_{C_1} = 0$.

We now prove that the ‘‘canonical’’ entangler Hamiltonian

$$H_{C_1}^{t-J} = - \sum_{i \neq j} \Delta_i^\dagger \Delta_j + h. c. \quad (17)$$

proposed in ref. 25 has the property that its ground-state is Eq. (16). We begin by observing that the Hamiltonian (17) conserves the number of electrons N in the physical and ancilla chains *separately*, and assume that the combined physical plus ancilla system has $S_z = 0$, so that the number of up and down electrons are equal in the combined system. Let us divide the full Hilbert space basis into ‘‘good states’’ where all physical sites and their ancillas are correctly paired, and ‘‘bad states’’ where at least one physical site is not correctly paired to its ancilla; these disjoint sets are then

$$\begin{aligned} \mathcal{S}_G &= \{|\phi\rangle; \text{basis } |\phi\rangle \text{ with all physical and ancilla} \\ &\quad \text{sites correctly paired}\} \\ \mathcal{S}_B &= \{|\phi\rangle; \text{basis } |\phi\rangle \text{ with at least one physical site} \\ &\quad \text{with ancilla incorrectly paired}\}. \end{aligned} \quad (18)$$

Note that if $|\phi\rangle \in \mathcal{S}_G$ then $|\phi\rangle$ is a term in Eq. (16). We shall prove that (i) $\langle \phi' | H_{C_1}^{t-J} | \phi \rangle = 0$ if $|\phi'\rangle \in \mathcal{S}_G$ and

$|\phi\rangle \in \mathcal{S}_B$, so that the Hamiltonian matrix $H_{C_1}^{t-J}$ blocks into at least two blocks: states in \mathcal{S}_G and states in \mathcal{S}_B . We shall furthermore prove (ii) that the ground state of $H_{C_1}^{t-J}$ is in the block \mathcal{S}_G as opposed to the block \mathcal{S}_B , and (iii) that the ground state of the block $\langle\phi'|H_{C_1}^{t-J}|\phi\rangle$ for all $|\phi\rangle, |\phi'\rangle \in \mathcal{S}_G$ is Eq. (16).

To prove (i) it suffices to think of Eq. (17) as a tight-binding Hamiltonian of “singlets” of physical sites and ancillas built along the rungs, singlets that are hopping along the ladder structure. Eq. (17) cannot connect states in \mathcal{S}_G with those in \mathcal{S}_B .

To prove (ii) we first note that if $|\phi\rangle \in \mathcal{S}_B$, then at least one site has occupation $|\sigma, 0\rangle$, $|0, \sigma\rangle$ or $|\sigma, \sigma\rangle$. Electrons in sites like these cannot “move” by the action of Eq. (17). The subspace \mathcal{S}_B then blocks into even smaller subspaces, all of size smaller than the set \mathcal{S}_G . Within these subspaces, we have hopping-like matrices yielding lowest energies larger than that of the block \mathcal{S}_G .

To prove (iii), let us call H the block of matrix Eq. (17) in the \mathcal{S}_G subspace. The Hamiltonian Eq. (17) conserves the number of electrons in the physical system, but not its total spin, so can be written in a tridiagonal block form. The diagonal blocks have rank $C_{N_\uparrow}^L C_{N-N_\uparrow}^{L-N_\uparrow}$ each, and are characterized by the number of up electrons. The blocks in the first diagonal above (below) the main diagonal connect states with N_\uparrow and $N_\uparrow + 1$ ($N_\uparrow - 1$) electrons and are given by $m \times n$ rectangular matrices with $m = C_{N_\uparrow}^L C_{N-N_\uparrow}^{L-N_\uparrow}$ and $n = C_{N_\uparrow+1}^L C_{N-N_\uparrow-1}^{L-N_\uparrow-1}$ ($n = C_{N_\uparrow-1}^L C_{N-N_\uparrow+1}^{L-N_\uparrow+1}$).

Now, the matrix elements in the blocks described above are either 0 or -1 for the diagonal blocks while for the off-diagonal ones are 0 and +1. Each row has exactly $2N(L-N)$ non-zero entries. So does each column. Then its lowest eigenvalue (by taking into account the factor $\sqrt{2}$ in the definition of the Δ operators) is $-N(L-N)$, with eigenstate $(1, 1, \dots, 1)$, that is, Eq. (16).

Because the $t-J$ chain has charge and spin degrees of freedom, there is an alternative and more efficient way of performing the canonical purification scheme: Consider the maximally entangled infinite temperature state

$$|\psi(\beta=0)\rangle_{C_2} = P_{\left(\begin{smallmatrix} N_{\text{ph.}}=N \\ S_{\text{ph.}}^z=0 \end{smallmatrix}\right)} \left[\bigotimes_{i=0}^{L-1} (|0,0\rangle + \sum_{\sigma=\uparrow,\downarrow} |\sigma\bar{\sigma}\rangle) \right], \quad (19)$$

where the projector operator is such that the total number of electrons *and* the total z -component of the physical (ancilla) chain are conserved,

$$N_{\text{ph.}}|\psi(\beta=0)\rangle_{C_2} = N|\psi(\beta=0)\rangle_{C_2} \quad (20)$$

$$N_{\text{an.}}|\psi(\beta=0)\rangle_{C_2} = N|\psi(\beta=0)\rangle_{C_2} \quad (21)$$

$$S_{\text{ph.}}^z|\psi(\beta=0)\rangle_{C_2} = S_{\text{an.}}^z|\psi(\beta=0)\rangle_{C_2} = \emptyset. \quad (22)$$

With a procedure similar to the one just outlined, it is possible to show that an “entangler” Hamiltonian yield-

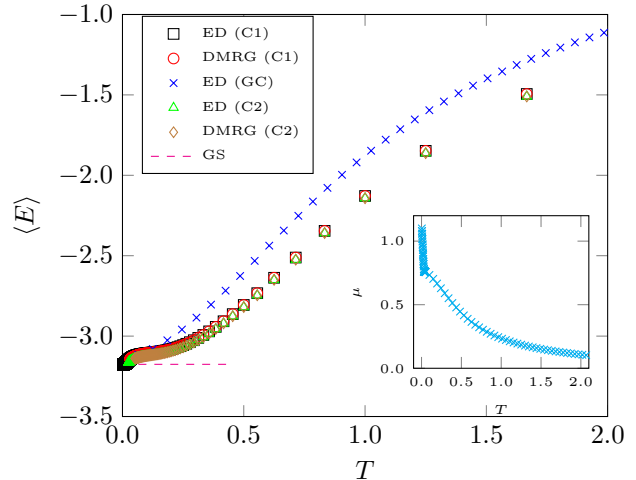


FIG. 3: (Color online) Intensive energies for a t-J chain of $L = 6$ sites, $N = 4$ electrons, with $J = 0.1$, for the canonical and grand canonical approaches (C1 and C2, see main text), and comparing DMRG against ED, as indicated. *Inset*: Chemical potential as a function of the temperature, calculated in the grand canonical approach so that the average density is always $N = 4$ electrons.

ing Eq. (19) as ground state is

$$H_{C_2}^{t-J} = - \sum_{\substack{i \neq j \\ \sigma = \uparrow, \downarrow}} c_{i,\sigma}^\dagger c_{i,\bar{\sigma}}^\dagger c_{j,\bar{\sigma}} c_{j,\sigma} + \text{h. c.} \quad (23)$$

The ground state energy of the above Hamiltonian is equal to $-N(L-N)$, coinciding with the result for the C1 Hamiltonian. Notice that, for an L site chain, the subspace containing the maximally entangled state in the canonical approach C1 has dimension $D_{C_1} = \sum_{N_\uparrow=0}^N C_{N_\uparrow}^L C_{N-N_\uparrow}^{L-N_\uparrow}$, which is evidently larger than the analogous subspace dimension $D_{C_2} = C_{N/2}^L C_{N/2}^{L-N/2}$ of the case C2, where one has also $N_\uparrow = N_\downarrow = N/2$. If one imposes the conservation of $N_{\text{ph.}}$ and $S_{\text{ph.}}^z$ during the finite temperature evolution in the enlarged Hilbert space, this remarkably reduces the computational effort and increases the efficiency of the time dependent DMRG simulations. In our typical runs, when this purification scheme is adopted, the computational time needed for obtaining the thermodynamic properties is reduced by a factor of two with respect to the canonical purification C1.

Fig. 3 shows the average intensive energy as a function of the temperature for a t-J chain with $L = 6$ sites, $N = 4$ electrons, and $J = 0.1$, ($t = 1$ is assumed as unit of energy) comparing canonical and grand canonical approaches. One observes a perfect numerical agreement between DMRG and ED for both canonical approaches C1 and C2. For the small system size considered, the results for the average energies differ (by less than 1%) at temperature larger than zero, while converging to the

ground state value in the limit of large β . We have verified that, even for a system size of $L = 12$ sites, the numerical results obtained in the C1 and C2 approaches are coincident within the numerical precision of our runs.

The results obtained in the grand canonical approach were calculated with ED by performing a procedure similar to a standard Maxwell construction. We first calculated the total electronic density as a function of the temperature, for different chemical potential values μ . By solving an equation similar to Eq. (15), $\langle N_{tot} \rangle = 4$, we have then extracted the chemical potential curve at constant density as function of the temperature, which is reported in the inset of fig. 3. Finally, in the main plot of fig. 3, the blue crosses represent the intensive energy as a function of the temperature. Even for small system sizes, DMRG calculations in the grand canonical approach are already computationally expensive. We can then conclude that the canonical purification C2 should be the computationally preferred choice for the study of the thermodynamic properties of the $t - J$ model. (Yet the disadvantages of the canonical are discussed in section III.)

C. Hubbard chains

1. Grand canonical purification scheme

In this section, we apply the purification schemes introduced in the previous section to a one dimensional Hubbard model described by the standard Hamiltonian

$$H_{Hub} = -t \sum_{i=0}^{L-2} (c_{i,\sigma}^\dagger c_{i+1,\sigma} + h.c.) + U \sum_{i=0}^{L-1} N_{i,\uparrow} N_{i,\downarrow}. \quad (24)$$

The model is characterized by a local four-dimensional Hilbert space with states empty $|0\rangle$, single occupied $|\uparrow\rangle$, $|\downarrow\rangle$ and double occupied $|\uparrow\downarrow\rangle$.

We start by considering the grand-canonical purification scheme. Following the same procedure used for the $t - J$ case, one can straightforwardly write (up to a constant)

$$|\psi\rangle = \bigotimes_{i=0}^{L-1} \left[|0, 0\rangle + |\uparrow\downarrow, \uparrow\downarrow\rangle + \sum_{\sigma=\uparrow,\downarrow} |\sigma\bar{\sigma}\rangle \right] \quad (25)$$

for the infinite temperature state in the grand canonical approach. The only difference with respect to the state Eq. (13) is that the double occupied state on a physical site is “mapped” to the same state on its ancilla. By diagonalizing a 16×16 matrix, where 16 is the dimension of a composite physical-plus-ancilla site, the state above can be generated by calculating the ground state of the entangler Hamiltonian

$$H_{GC}^{\text{Hubbard}} = \sum_{i=0, \sigma=\uparrow,\downarrow}^{L-1} (c_{i,\sigma} c_{a(i),\bar{\sigma}} P_i^\sigma + h. c.), \quad (26)$$

where $P_i^\sigma = |1 - N_{i,\bar{\sigma}} - N_{a(i),\sigma}\rangle$.

State Eq. (25) conserves the total spin in the enlarged chain, but does not do so for the physical chain. A chemical potential μ must therefore be added in the Hamiltonian used during the temperature evolution, and *mutatis mutandis*, the same procedure outlined in the previous section for the $t - J$ case must be followed. The average total spin of the physical chain is zero at any temperature, that is, $\langle \psi(\beta, \mu) | S_{tot}^z | \psi(\beta, \mu) \rangle = 0$, with μ being a solution of an equation similar to Eq. (15). Because of the computational cost of the procedure, the results in the grand canonical scheme are presented using only exact diagonalization on a small system size.

2. Canonical purification scheme

We now address the “canonical” purification schemes for the Hubbard model. We consider a chain with L sites, filling N/L , and a total even number of electrons N , such that $N_\uparrow = N_\downarrow = N/2$.

Up to a constant, the “canonical” maximally entangled state of type C1 at infinite temperature is

$$|\psi\rangle_{C1} = P_{(N_{\text{ph.}}=N)} \left[\bigotimes_{i=0}^{L-1} (|0, 0\rangle + |\uparrow\downarrow, \uparrow\downarrow\rangle + \sum_{\sigma=\uparrow,\downarrow} |\sigma\bar{\sigma}\rangle) \right], \quad (27)$$

where $P_{(N_{\text{ph.}}=N)}$ is a projector operator such that the total number of electrons of the physical (ancilla) chain is conserved,

$$N_{\text{ph.}} |\psi_{\beta=0}\rangle_{C1} = N_{\text{an.}} |\psi_{\beta=0}\rangle_{C1} = N |\psi_{\beta=0}\rangle_{C1}. \quad (28)$$

Even though this state conserves charge in the physical chain, it does *not* conserve the z -component of the spin of the physical chain. Yet, ${}_{C1} \langle \psi(\beta) | S_{\text{ph.}}^z | \psi(\beta) \rangle_{C1} = 0$.

As shown below, the canonical purification just discussed is not the most efficient for a DMRG implementation. For this reason, in the rest of the section we focus on the canonical scheme of type C2: the maximally entangled infinite temperature state

$$|\psi\rangle_{C2} = P_{\left(\begin{smallmatrix} N_{\text{ph.}}=N \\ S_{\text{ph.}}^z=0 \end{smallmatrix}\right)} \left[\bigotimes_{i=0}^{L-1} (|0, 0\rangle + |\uparrow\downarrow, \uparrow\downarrow\rangle + \sum_{\sigma=\uparrow,\downarrow} |\sigma\bar{\sigma}\rangle) \right], \quad (29)$$

where the projector operator is such that the total number of electrons *and* the total z -component of the physical (ancilla) chain are conserved,

$$\begin{aligned} N_{\text{ph.}} |\psi_{\beta=0}\rangle_{C2} &= N_{\text{an.}} |\psi_{\beta=0}\rangle_{C2} = N |\psi_{\beta=0}\rangle_{C2}, \\ S_{\text{ph.}}^z |\psi_{\beta=0}\rangle_{C2} &= S_{\text{an.}}^z |\psi_{\beta=0}\rangle_{C2} = \emptyset. \end{aligned} \quad (30)$$

With a procedure similar to that outlined in section II B 2, it is possible to show (see appendix C) that an “entangler” Hamiltonian giving Eq. (29) as ground state is

$$H_{C2}^{\text{Hubbard}} = - \sum_{\substack{i \neq j \\ \sigma=\uparrow,\downarrow}} \Lambda_{\sigma,i}^\dagger \Lambda_{\sigma,j} + h. c., \quad (31)$$

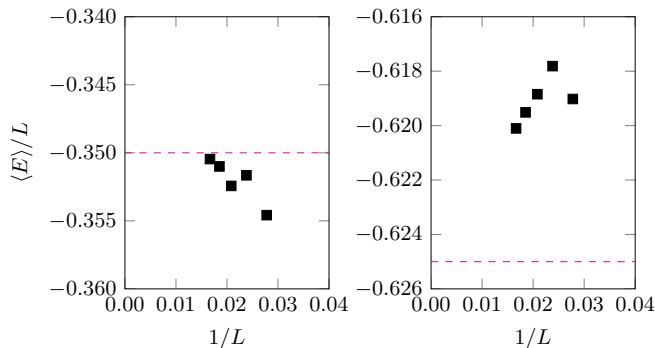


FIG. 4: (Color online) Intensive energies for the Hubbard model, $U = 10$, and density $2/3$, as a function of the system size. Squares indicate data obtained with DMRG using a maximum of $m = 1000$ and a truncation error of 10^{-6} . The dashed (magenta) lines indicate the energy calculated with thermodynamic Bethe ansatz. Left panel shows $T = 1.25$, right panel $T = 0.25$.

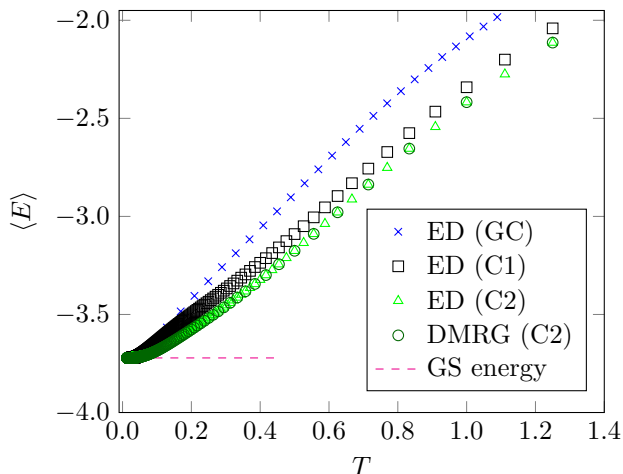


FIG. 5: (Color online) Intensive energies for the Hubbard model, $U = 10$, and density $2/3$, as a function of the temperature for a $L = 6$ chain. Shown are results within the grand canonical, calculated using ED, blue crosses; canonical C1, calculated using ED, black squares; canonical C2 calculated using ED, green triangles; and canonical C2 obtained with DMRG, dark green empty circles. The ground state solution is also indicated with a magenta dashed line.

where $\Lambda_{i,\sigma} = c_{i,\sigma} c_{i,\sigma} P_i^\sigma$, where P_i^σ is given below Eq. (26).

For an L site chain, the subspace containing the maximally entangled state in the canonical approach C1 has dimension $D_{C1} = \sum_{N_\uparrow=0}^N C_{N_\uparrow}^L C_{N_\uparrow}^L$, which is larger than the analogous subspace dimension $D_{C2} = C_{N/2}^L C_{N/2}^L$ of the case C2; both cases have $N_\uparrow = N_\downarrow = N/2$. (Notice the difference with the corresponding expressions provided for the $t - J$ model in the previous section.) If one imposes the conservation of N_{ph} , and S_{ph}^z , during

the finite temperature evolution in the enlarged Hilbert space, one can thus reduce (in our typical runs by a factor of two or more) the computational time needed for obtaining the thermodynamic properties. We therefore recommend that the canonical approach C2 be the preferred purification scheme when finite temperature static and even dynamic properties are calculated with DMRG.

Figure 4 shows the intensive energies as a function of the system size for the canonical approach C2 for $U = 10$ ($t = 1$ is assumed as unit of energy) and filling $2/3$. The left panel shows data at $T = 1.25$, while the right panel at $T = 0.25$. Using $m = 1000$ and imposing a truncation error not bigger than 10^{-6} in the DMRG runs, the results get closer to the thermodynamic Bethe ansatz results as the system size increases. In this paper, we have considered chains of length up to $L = 60$.

Fig. 5 shows a comparison between the intensive energies obtained in the canonical and grand canonical approaches for a Hubbard chain with $L = 6$ sites, $N = 4$ electrons, and $U = 10$ as a function of temperature. Because the system size is small, the numerical results differ in the three approaches, even though they converge to the exact ground state solution in the limit of $\beta \rightarrow \infty$. Remarkably, even for $L = 6$, the results of the C1 and C2 approaches differ by less than 5% on the entire β interval studied.

For the canonical purification scheme C2, Fig. 5 also compares DMRG results against those obtained with ED. The agreement is close to the numerical precision. Finally, the computationally expensive results with the grand canonical approach are also shown. These results are calculated by performing a procedure similar to a standard Maxwell construction.

III. LONG RANGE INTERACTIONS IN CANONICAL ENTANGLERS

In this section, we discuss the properties of the entangler Hamiltonians in the canonical purification scheme. As already mentioned in the previous sections, the entangler Hamiltonians have long range interactions, with connections between sites at all possible distances. The resulting entanglement growth makes it difficult to compute the ground state of such Hamiltonians with the DMRG. Therefore, one would think that the grand canonical approach, where the *local* entangler Hamiltonians are used, would be more efficient for the calculation of the thermodynamic quantities. But the canonical purification scheme is computationally much more efficient.

Fig. 6 explains why. It shows the CPU times of the two purification schemes for the Heisenberg model. CPU times are divided in two parts: the calculation of the ground state of the entangler Hamiltonian (black bars), and temperature evolution up to the desired inverse temperature $\beta = 0.8$ (gray (red) bars), starting from the ground state of the entangler Hamiltonian. The computational time needed to calculate the ground state of the

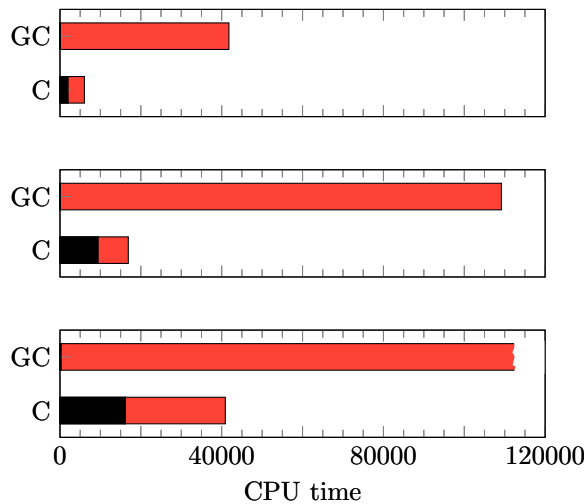


FIG. 6: (Color online) CPU time (in seconds) of typical runs in the grand canonical and grand canonical approaches for the Heisenberg model at $\beta = 0.8$, $J = -1$, and different system sizes. The black bars indicate the CPU time needed to solve the entangler Hamiltonian (for the GC see Eq. (6), for C see Eq. (9)), while the red bars indicate the same quantity for the temperature evolution. In the top panel ($L = 24$) and middle panel ($L = 48$) $m = 400$ DMRG states are used for the temperature evolution, while in the bottom panel ($L = 64$) $m = 600$. The CPU time for GC with $L=64$ has been truncated (the actual value is 595,000), because it is larger than the maximum CPU time shown in this scale.

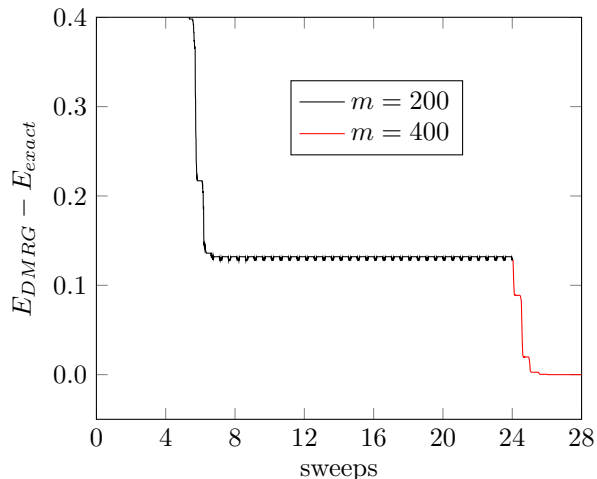


FIG. 7: (Color online) Difference between the ground state energy of the entangler Hamiltonian Eq. (31) for the Hubbard model at density $2/3$ and the exact ground state energy as a function of the number of DMRG sweeps. A chain with $L = 60$ sites is considered. Increasing the number of DMRG states kept from $m = 200$ to $m = 400$ allows the results to converge to the exact ground state energy.

entangler in the grand canonical approach is too small to be visible in the figure. The CPU time needed for the canonical entangler Hamiltonian is larger and visible as black bars. The *apparent* disadvantage of the canonical purification versus the grand canonical scheme seems to increase if large system sizes are considered. For $L = 64$ sites and $m = 200$, the CPU time needed in the canonical scheme for the ground state calculation is about three orders of magnitude longer than that needed in the grand canonical approach.

As indicated by the gray (red) bars in Fig. 6, the CPU time of the temperature evolution of the canonical purification is remarkably smaller than that of the grand canonical, because the temperature evolution takes place in a Hilbert space of reduced dimensions. (This results from the conservation of S_{ph}^z , as stated in sec. II A.) Given that the total CPU time is equal to the sum of the CPU time needed for the entangler plus the CPU time needed for the temperature evolution, we can conclude that the canonical purification scheme is faster than the grand canonical approach—by one order of magnitude or more.

Yet it is important to make sure that ground states of canonical entanglers are converged, given the aforementioned difficulties due to the long range interactions. To that aim, Fig. 7 is an example showing that the canonical entanglers used throughout this paper are converged. Fig. 7 shows the ground state energy of the canonical entangler C2 for the Hubbard model as a function of the number of DMRG sweeps, for a chain of $L = 60$ sites with $U = 10$ and density $2/3$. Several sweeps and two values of m were used to converge to the exact ground state.

We end this section by providing the ground state energies of the entangler Hamiltonians. Let L be the number of physical sites of the system. As shown in Appendix B, the ground state energy of the Heisenberg entangler Eq. 9 is $-L^2/4$. Let N be the number of electrons in the physical system. Section II.B.2 shows that the ground state energy of the t-J entangler Eq. (17) is $-N(L-N)$, which is equal to that of Eq. (23). Appendix C proves that the ground state energy of the Hubbard entangler Eq. (31) is $-N(L-N/2)$.

IV. SUMMARY AND CONCLUSIONS

In summary, we have improved the efficiency of the ancilla method for finite temperature DMRG by employing the *inherent* symmetries of the physical system in consideration. We have designed different entangler Hamiltonians to obtain infinite temperature states to use as starting states for the temperature evolution. Table I reports the purification schemes adopted for each model considered, and serves as an index to the equations obtained. The supplemental material³⁹ provides a pointer to the full open source code, input decks and additional computational details.

As a main result, we have derived entangler Hamiltoni-

ans for the canonical purification scheme of spin chains, the $t - J$ model and the Hubbard model. The present work codifies an efficient ancilla method for spin chains and fermionic systems, because (i) canonical purification is the most efficient for obtaining the thermodynamic properties of the physical system in consideration, and (ii) entangler Hamiltonians are needed to obtain workable representations of infinite temperature states. Moreover, the efficiency brought about by the use of symmetries does not compromise accuracy: the ancilla method is as accurate as originally proposed.

Due to their long range interactions, canonical entanglers appear computationally costlier than grand canonical ones. But grand canonical entanglers have to be simulated on larger Hilbert spaces. *Overall, canonical entanglers turn out to be computationally much more efficient*, as was shown in section III.

In the Hubbard model away from half-filling, we have verified that the efficiency gain of the canonical scheme overcomes the extra cost due to the need for more states in the temperature evolution for small and medium-size systems (up to $L = 60$). For very large system sizes and at half filling, the grand canonical approach remains an alternative method for the calculation of the thermodynamic properties⁴². Yet the grand canonical scheme away from half-filling requires computational runs to adjust the chemical potential at every temperature!

The purification schemes proposed are general and can be applied to both more complex one dimensional models and to geometries beyond chains. They apply to more general models because the Hamiltonian of the system comes into play only in the temperature evolution. They apply to more general geometries because the ancillas can be thought of as an extra orbital for each physical one.

Concerning the Hubbard and t - J models, we believe that the canonical approach C2 should be the preferred purification scheme when finite temperature static and even dynamic properties are calculated with DMRG. For instance, in ref. 28, the entanglement growth characterizing the purification scheme has been reduced by time evolving the auxiliary degrees of freedom backward in time, when a combination of finite temperature and time

N_e^{ph}	S_z^{ph}	Heisenberg	t - J Model	Hubbard
No	No		GC, (13), (14)	GC, (25), (26)
Yes	No	GC, (5), (6)	C1, (13), (17)	C1, (27)
Yes	Yes	C, (8), (9)	C2, (19), (23)	C2, (29), (31)

TABLE I: For each row, the conservation of the number of particles N_e^{ph} or number of particles N_e^{ph} and the z component of the spin S_z^{ph} of the physical system is indicated by “Yes” or “No.” For each model, the labels grand canonical (GC), canonical type 1 (C1) or type 2 (C2) are defined. The numbers refer to equations in this paper: the first number is the equation defining the infinite temperature state, the second number (if present) is the equation defining the corresponding *entangler* Hamiltonian. For the Heisenberg model the N_e^{ph} column should be ignored.

dependent DMRG is needed for the calculation of spectral properties. We think that a natural step would be to combine the suggested improvement with the canonical purification proposed in this paper.

Acknowledgments

We would like to thank T. Barthel, E. Dagotto, A. Feiguin, C. Karrasch, S. Manmana, U. Schollwöeck, and M. Stoudenmire for helpful discussions and suggestions. This work was conducted at the Center for Nanophase Materials Sciences, sponsored by the Scientific User Facilities Division, Basic Energy Sciences, U.S. Department of Energy, under contract with UT-Battelle. We acknowledge support by the early career research program, DSUF, BES, DOE.

Appendix A: Canonical vs. grand canonical ensemble

The purpose of this appendix is three-fold. First, to show that, for finite systems at finite temperature, the canonical and grand canonical ensembles do not, in general, yield the same averages. Second, to show that, at $T = 0$, the canonical and grand canonical ensembles agree for any Hamiltonian. And third, that they also agree *in the thermodynamic limit* for any Hamiltonian. Even though these results are known, we prove them below for completeness.

Observation 1. *At finite temperature, there exists at least one finite dimensional Hamiltonian with canonical average energy different than its grand canonical average energy.*

Proof. We construct such a Hamiltonian by considering 2 levels, and a one-site Hilbert space including the states, empty, level 1 occupied only, level 2 occupied only, and both levels occupied. Let

$$H = \epsilon(\hat{n}_1 + \hat{n}_2) + V\hat{n}_1\hat{n}_2, \quad (\text{A1})$$

where \hat{n}_l acting on the basis states multiplies it by the level l occupation of that state. Let $\epsilon > 0$ and $V > 0$. The average energy in the canonical ensemble with exactly $N = 1$ particle in the system is $\langle E \rangle_C = \epsilon$. The average energy in the grand-canonical ensemble with density $\langle N \rangle = 1$ is given by $\langle E \rangle_{GC} = \epsilon + \frac{V/2}{1+e^{\beta V/2}}$, which is greater than ϵ at finite temperature. \square

Observation 2. *For any finite dimensional Hamiltonian with convex energies, at zero temperature, the average energy in the canonical ensemble is the same as the one in the grand canonical ensemble.*

Proof. Let us consider a system with M sites and target density N_T . The number M includes sites, orbitals and spin, such that the maximum number of electrons that

the system can hold is M . Let the eigenvalues of the Hamiltonian be $E_{n'}^N$, where the index n' runs only over states of Fock sector \mathcal{F}_N of N particles. Let $E_{\min}^N = \min_{n' \in \mathcal{F}_N} E_{n'}^N$. At $T = 0$, the average energy in the canonical ensemble with density N_T is $E_{\min}^{N_T}$. In the grand canonical (GC) ensemble we impose $\langle N \rangle_{GC, T=0} = N_T$, and thus the chemical potential μ is obtained by imposing that the N that minimizes $F_N \equiv E_{\min}^N - \mu N$ be N_T . Because the energies are convex, such a μ is unique. For this μ , we obtain $\langle E \rangle_{GC, T=0} = E_{\min}^{N_T}$, which coincides with the canonical result. \square

Observation 3. *For any Hamiltonian with convex energies and an extensive canonical partition function, at finite temperature, and in the thermodynamic limit, the average energy in the canonical ensemble is the same as the one in the grand canonical ensemble.*

Proof. The proof is given in the supplemental material.³⁹ \square

Appendix B: Canonical entangler for the Heisenberg model

We now prove that the ‘‘canonical’’ entangler Hamiltonian for the Heisenberg model, Eq. (9), has the property that its ground-state is Eq. (8). We begin by observing that the Hamiltonian (9) conserves the z -component of the total spin in the physical and ancilla chains *separately*, and assume that the combined physical plus ancilla system has $S_z = 0$, so that the number of up and down spins are equal in the combined system. Let

$$\begin{aligned} \mathcal{T}_G &= \{|\phi\rangle; \text{basis } |\phi\rangle \text{ with all physical and ancilla} \\ &\quad \text{sites correctly paired}\} \\ \mathcal{T}_B &= \{|\phi\rangle; \text{basis } |\phi\rangle \text{ with at least one physical site} \\ &\quad \text{with ancilla incorrectly paired}\}, \end{aligned} \quad (\text{B1})$$

where \mathcal{T}_G is the set of states in which each site is correctly paired with ancilla according to the scheme $\uparrow \rightarrow \downarrow$, $\downarrow \rightarrow \uparrow$, and \mathcal{T}_B the set where at least one site is incorrectly paired.

It is easy to prove (i) that $\langle \phi' | H_C^{spin} | \phi \rangle = 0$ if $|\phi'\rangle \in \mathcal{T}_G$ and $|\phi\rangle \in \mathcal{T}_B$, so that the Hamiltonian matrix H_C^{spin} blocks into at least two blocks: states in \mathcal{T}_G and states in \mathcal{T}_B . To this aim, it is sufficient to think of spins as mapped to hard-core bosons, $|\uparrow\rangle = |1\rangle$ $|\downarrow\rangle = |0\rangle$. One can imagine Eq. (9) as a tight-binding Hamiltonian of ‘‘singlets’’ of physical sites and ancillas built along the rungs, singlets that are exchanging positions of particles and holes. Because Eq. (9) conserves the number of bosons in the physical and ancilla chain separately, it cannot, therefore, connect states in \mathcal{T}_G (number of bosons and holes is equal to $L/2$ in the physical chain) with those in \mathcal{T}_B . In fact, in the subspace \mathcal{T}_B at least one site of the chain has, in the hard-core bosonic representation, occupation $|0, 0\rangle$ ($|\downarrow, \downarrow\rangle$), $|1, 1\rangle$ ($|\uparrow, \uparrow\rangle$), bosons in

sites like these cannot ‘‘move’’ by the action of Eq. (9). As in the other cases, the subspace \mathcal{T}_B then blocks into even smaller subspaces, all of size smaller than the set \mathcal{T}_G . Within these subspaces we have hopping-like matrices yielding lowest energies which are larger than those in the set \mathcal{T}_G .

To prove (iii), let us call H the block of matrix Eq. (9) in the \mathcal{T}_G subspace. The rank of H is $C_{L/2}^L$ and its matrix elements are either 0 or -1. Each row has exactly $L^2/4$ non-zero entries. So does each column. Then its lowest eigenvalue is $-L^2/4$, with eigenstate $(1, 1, \dots, 1)$, that is, Eq. (8).

Appendix C: Canonical entangler for the Hubbard model

We now prove that the ‘‘canonical’’ entangler Hamiltonian of type C2 for the Hubbard model, Eq. (31), has the property that its ground-state is Eq. (29). We begin by observing that the Hamiltonian (31) conserves the number of electrons and z -component of the total spin in the physical and ancilla chains *separately*, and assume that the combined physical plus ancilla system has $S_z = 0$, so that the number of up and down electrons are equal in the combined system. As done in Eq. 18, let

$$\begin{aligned} \mathcal{W}_G &= \{|\phi\rangle; \text{basis } |\phi\rangle \text{ with all physical and ancilla} \\ &\quad \text{sites correctly paired}\} \\ \mathcal{W}_B &= \{|\phi\rangle; \text{basis } |\phi\rangle \text{ with at least one physical site} \\ &\quad \text{with ancilla incorrectly paired}\}, \end{aligned} \quad (\text{C1})$$

where \mathcal{W}_G is the set of states in which each site is correctly paired with ancilla according to the scheme $0 \rightarrow 0$, $\uparrow \rightarrow \downarrow$, $\downarrow \rightarrow \uparrow$, $\uparrow \downarrow \rightarrow \uparrow \downarrow$, and \mathcal{W}_B the set where at least one site is incorrectly paired.

Even in this case, it is easy to prove (i) that $\langle \phi' | H_{C2}^{Hub} | \phi \rangle = 0$ if $|\phi'\rangle \in \mathcal{W}_G$ and $|\phi\rangle \in \mathcal{W}_B$, so that the Hamiltonian matrix H_{C2}^{Hub} blocks into at least two blocks: states in \mathcal{W}_G and states in \mathcal{W}_B . Indeed, it is sufficient to imagine Eq. (31) as a tight-binding Hamiltonian of generalized ‘‘singlets’’ of physical sites and ancillas built along the rungs

$$|\psi_{\text{rungsinglet}}\rangle = |0, 0\rangle + |\uparrow \downarrow, \uparrow \downarrow\rangle + |\uparrow, \downarrow\rangle + |\downarrow, \uparrow\rangle. \quad (\text{C2})$$

Because Eq. (31) conserves the number of electrons in the physical and ancilla chain separately, it cannot, therefore, connect states in \mathcal{W}_G with those in \mathcal{W}_B . In fact, in the subspace \mathcal{W}_B at least one site of the chain has occupation $|\sigma, 0\rangle$, $|0, \sigma\rangle$, $|\uparrow \downarrow, \sigma\rangle$, $|\sigma, \uparrow \downarrow\rangle$ or $|\sigma, \sigma\rangle$. Electrons in sites like these cannot ‘‘move’’ by the action of Eq. (31). As in the other cases, the subspace \mathcal{W}_B then blocks into even smaller subspaces, all of size smaller than the set

\mathcal{W}_G . Within these subspaces we have hopping-like matrices yielding lowest energies which are larger than those in the set \mathcal{W}_G .

To prove (iii), let us call H the block of matrix Eq. (31) in the \mathcal{S}_G subspace. It can be written as a direct product $H = H_\uparrow \otimes H_\downarrow$. $H_\uparrow = H_\downarrow$, each has rank $C_{N/2}^L$, and

matrix elements either 0 or -1. Each row has exactly $N(L - N/2)/2$ non-zero entries. So does each column. Then the lowest eigenvalue of H is $-N(L - N/2)$, with eigenstate $(1, 1, \dots, 1)$, that is, Eq. (29).

-
- ¹ S. Sachdev, *Quantum phase transitions* (Wiley Online Library, 2007).
- ² G. A. Fiete, Rev. Mod. Phys. **79**, 801 (2007), URL <http://link.aps.org/doi/10.1103/RevModPhys.79.801>.
- ³ A. J. A. James, W. D. Goetze, and F. H. L. Essler, Phys. Rev. B **79**, 214408 (2009), URL <http://link.aps.org/doi/10.1103/PhysRevB.79.214408>.
- ⁴ S. E. Nagler, W. J. L. Buyers, R. L. Armstrong, and B. Briat, Phys. Rev. B **28**, 3873 (1983), URL <http://link.aps.org/doi/10.1103/PhysRevB.28.3873>.
- ⁵ J. Villain, Physica B+C **79**, 1 (1975), ISSN 0378-4363, URL <http://www.sciencedirect.com/science/article/pii/0378436375901011>.
- ⁶ Y. Zhu, *Modern techniques for characterizing magnetic materials* (Springer Science & Business Media, 2005).
- ⁷ B. Lake, D. A. Tennant, C. D. Frost, and S. E. Nagler, Nat. Mater. **4**, 329 (2005), URL <http://dx.doi.org/10.1038/nmat1327>.
- ⁸ G. Xu, C. Broholm, Y.-A. Soh, G. Aeppli, J. F. DiTusa, Y. Chen, M. Kenzelmann, C. D. Frost, T. Ito, K. Oka, et al., Science **317**, 1049 (2007), <http://www.sciencemag.org/content/317/5841/1049.full.pdf>, URL <http://www.sciencemag.org/content/317/5841/1049.abstract>.
- ⁹ S. A. Zvyagin, Low Temperature Physics **38**, 819 (2012), URL <http://scitation.aip.org/content/aip/journal/ltp/38/9/10.1063/1.4752094>.
- ¹⁰ S. Grossjohann and W. Brenig, Phys. Rev. B **79**, 094409 (2009), URL <http://link.aps.org/doi/10.1103/PhysRevB.79.094409>.
- ¹¹ A. W. Sandvik and J. Kurkijärvi, Phys. Rev. B **43**, 5950 (1991), URL <http://link.aps.org/doi/10.1103/PhysRevB.43.5950>.
- ¹² A. W. Sandvik, AIP Conference Proceedings **1297**, 135 (2010), URL <http://scitation.aip.org/content/aip/proceeding/aipcp/10.1063/1.3518900>.
- ¹³ S. R. White, Phys. Rev. Lett. **69**, 2863 (1992), URL <http://link.aps.org/doi/10.1103/PhysRevLett.69.2863>.
- ¹⁴ S. R. White, Phys. Rev. B **48**, 10345 (1993), URL <http://link.aps.org/doi/10.1103/PhysRevB.48.10345>.
- ¹⁵ U. Schollwöck, Annals of Physics **326**, 96 (2011), ISSN 0003-4916, January 2011 Special Issue, URL <http://www.sciencedirect.com/science/article/pii/S0003491610001752>.
- ¹⁶ A. E. Feiguin and S. R. White, Phys. Rev. B **72**, 220401 (2005), URL <http://link.aps.org/doi/10.1103/PhysRevB.72.220401>.
- ¹⁷ A. J. Daley, C. Kollath, U. Schollwöck, and G. Vidal, Journal of Statistical Mechanics: Theory and Experiment **2004**, P04005 (2004), URL <http://stacks.iop.org/1742-5468/2004/i=04/a=P04005>.
- ¹⁸ G. Vidal, Phys. Rev. Lett. **93**, 040502 (2004), URL <http://link.aps.org/doi/10.1103/PhysRevLett.93.040502>.
- ¹⁹ P. Schmitteckert, Phys. Rev. B **70**, 121302 (2004), URL <http://link.aps.org/doi/10.1103/PhysRevB.70.121302>.
- ²⁰ J. Sirker and A. Klümper, Phys. Rev. B **71**, 241101 (2005), URL <http://link.aps.org/doi/10.1103/PhysRevB.71.241101>.
- ²¹ S. R. White, Phys. Rev. Lett. **102**, 190601 (2009), URL <http://link.aps.org/doi/10.1103/PhysRevLett.102.190601>.
- ²² E. M. Stoudenmire and S. R. White, New Journal of Physics **12**, 055026 (2010), URL <http://stacks.iop.org/1367-2630/12/i=5/a=055026>.
- ²³ L. Bonnes, F. H. L. Essler, and A. M. Läuchli, Phys. Rev. Lett. **113**, 187203 (2014), URL <http://link.aps.org/doi/10.1103/PhysRevLett.113.187203>.
- ²⁴ T. Barthel, U. Schollwöck, and S. R. White, Phys. Rev. B **79**, 245101 (2009), URL <http://link.aps.org/doi/10.1103/PhysRevB.79.245101>.
- ²⁵ A. E. Feiguin and G. A. Fiete, Phys. Rev. B **81**, 075108 (2010), URL <http://link.aps.org/doi/10.1103/PhysRevB.81.075108>.
- ²⁶ F. Verstraete, J. J. García-Ripoll, and J. I. Cirac, Phys. Rev. Lett. **93**, 207204 (2004), URL <http://link.aps.org/doi/10.1103/PhysRevLett.93.207204>.
- ²⁷ M. Zwoleak and G. Vidal, Phys. Rev. Lett. **93**, 207205 (2004), URL <http://link.aps.org/doi/10.1103/PhysRevLett.93.207205>.
- ²⁸ C. Karrasch, J. H. Bardarson, and J. E. Moore, New Journal of Physics **15**, 083031 (2013), URL <http://stacks.iop.org/1367-2630/15/i=8/a=083031>.
- ²⁹ A. C. Tiegel, S. R. Manmana, T. Pruschke, and A. Honecker, Phys. Rev. B **90**, 060406 (2014), URL <http://link.aps.org/doi/10.1103/PhysRevB.90.060406>.
- ³⁰ G. Alvarez, Phys. Rev. B **87**, 245130 (2013), URL <http://link.aps.org/doi/10.1103/PhysRevB.87.245130>.
- ³¹ M. Binder and T. Barthel, arXiv:1411.3033 [cond-mat.str-el] (2014).
- ³² B. Bruognolo, J. von Delft, and A. Weichselbaum, arXiv:1506.03336 [cond-mat.str-el] (2015).
- ³³ H. Umezawa, H. Matsumoto, and M. Tachiki, *Thermo Field Dynamics and Condensed States* (North-Holland, Amsterdam, 1982).
- ³⁴ M. Suzuki, J. Phys. Soc. Jpn. **12**, 4483 (1985).
- ³⁵ Suzuki and Masuo, Journal of Statistical Physics **42**, 1047 (1986), ISSN 0022-4715, URL <http://dx.doi.org/10.1007/BF01010461>.
- ³⁶ Y. Takahashi and H. Umezawa, Collect. Phenom. **2**, 55 (1975).
- ³⁷ A. E. Feiguin and I. Klich, arXiv:1308.0756.
- ³⁸ I. P. McCulloch, Journal of Statistical Mechanics: Theory and Experiment **2007**, P10014 (2007).
- ³⁹ See Supplemental Material at [URL will be inserted by publisher] for a more detailed description of the numerical

data shown, and other computational details.

⁴⁰ S. R. Manmana, A. Muramatsu, and R. M. Noack, in *AIP Conf. Proc.*, edited by A. Avella and F. Mancini (2005), vol. 789, pp. 269–278, also in <http://arxiv.org/abs/cond-mat/0502396v1>.

⁴¹ G. Alvarez, L. G. G. V. Dias da Silva, E. Ponce, and

E. Dagotto, *Phys. Rev. E* **84**, 056706 (2011), URL <http://link.aps.org/doi/10.1103/PhysRevE.84.056706>.

⁴² C. Karrasch, D. M. Kennes, and J. E. Moore, *Phys. Rev. B* **90**, 155104 (2014), URL <http://link.aps.org/doi/10.1103/PhysRevB.90.155104>.